atmosphere

MDPI

Article

Clear-Air Turbulence over China: Climatology and Multiscale Mechanisms from First Long-Term Aircraft Reports

Wei Zhang [1,2], Xiaochen Zhang [2], Wei Yuan [2], Chongyu Zhang [2], Minghua Hu [1] and Ting Yang [3,*]

[1] College of Civil Aviation, Nanjing University of Aeronautics and Astronautics, Nanjing 211106, China; frogwei@atmb.net.cn (W.Z.); minghuahu@nuaa.edu.cn (M.H.)
[2] Aviation Meteorological Center of the Air Traffic Management Bureau, Civil Aviation Administration of China, Beijing 100710, China; zhangxiaochen@atmb.net.cn (X.Z.); yuanwei@atmb.net.cn (W.Y.); zhangchongyu@atmb.net.cn (C.Z.)
[3] State Key Laboratory of Atmospheric Environment and Extreme Meteorology, Institute of Atmospheric Physics, Chinese Academy of Sciences, Beijing 100029, China
* Correspondence: tingyang@mail.iap.ac.cn

Abstract

Clear-air turbulence (CAT), as a key meteorological hazard threatening aviation safety, urgently requires the revelation of its spatiotemporal distribution patterns and formation mechanisms within the China region. Based on the first release of 12,539 aircraft turbulence voice reports from China's civil aviation from 2022 to 2024 and ERA5 high-resolution reanalysis data, this study constructs for the first time a climatological portrait of aircraft turbulence over China, revealing the spatiotemporal distribution characteristics and formation mechanisms of CAT in the region: turbulence occurs predominantly at 3000–8000 m (accounting for 61.0%), peaking at 7000–8000 m, driven by strong low-level jet wind shear and Kelvin–Helmholtz instability (KHI); wintertime exhibits a high frequency (33.4%) stemming from strong upper-level jets (>30 m s^{-1}), while summer is dominated by low-level thermal convection (21.0%); the high-incidence zones of Central-South and Southwest China (>2800 events) are jointly governed by a mid-level strong horizontal gradient of vertical vorticity, divergence perturbations, and jet shear, with the winter jet shifting southward (22–30° N), further intensifying the turbulence risk. The findings establish a dynamic–thermodynamic coupling mechanism for CAT over China, providing a scientific basis for aviation safety early warning.

Keywords: clear-air turbulence (CAT); aviation safety; climatology; multiscale mechanisms

Academic Editor: Stephan De Wekker

Received: 31 August 2025
Revised: 24 September 2025
Accepted: 11 October 2025
Published: 21 October 2025

Citation: Zhang, W.; Zhang, X.; Yuan, W.; Zhang, C.; Hu, M.; Yang, T. Clear-Air Turbulence over China: Climatology and Multiscale Mechanisms from First Long-Term Aircraft Reports. *Atmosphere* **2025**, *16*, 1218. https://doi.org/10.3390/atmos16101218

1. Introduction

Clear-air turbulence (CAT) is a major meteorological hazard threatening aviation safety. Due to its occurrence in cloudless high altitudes, where there is a lack of visible water vapor condensation, it is difficult for onboard weather radar, which primarily detects water droplets, to identify it. Specialized equipment like Doppler lidar is often needed for detection. Its unpredictable nature frequently leads to passenger injuries, aircraft damage, and flight delays [1–3]. Global aviation growth and climate change are amplifying the latent risk of turbulence [4,5], making it urgent to understand in depth the spatiotemporal characteristics and causes of bumps to improve flight safety.

International studies have already used diverse data (Pilot Reports (PIREPs), Flight Data Recorder (FDR), and model output) to reveal the distribution patterns and key triggers (upper-level jet streams, strong vertical wind shear, and instability mechanisms) of

turbulence in the upper troposphere–lower stratosphere (UTLS) layer over different regions (North America [6], Europe [7], and East Asia [1]). Yet, for China, an airspace with dense traffic and distinctive meteorological conditions (e.g., the Tibetan Plateau, the East Asian monsoon, and powerful westerly jets), systematic climatological research based on long-term multi-source observations (especially voice reports) and its comprehensive relationship with upper-air dynamic and thermal fields remains scarce [8,9].

This study aims to fill this gap. Using 2022–2024 Chinese civil-aviation aircraft voice turbulence reports together with high-resolution ERA5 reanalysis, we present the first systematic depiction of the spatiotemporal characteristics (altitude, season, and spatial distribution) of turbulence over China. We focus on analyzing the physical links and synergistic mechanisms between high-incidence regions (e.g., Central-South and Southwest China) and seasons (e.g., winter) and key meteorological factors (jet streams, wind shear, stratification stability, turbulence index MOS CAT (the turbulence prediction factor), vorticity/divergence fields, temperature advection, et al.). The work constructs a detailed climatological picture of CAT over China, clarifies its multi-scale dynamic–thermodynamic causes, and provides scientific support for improving monitoring and early warning as well as for optimizing route planning.

2. Data and Methods

2.1. Data Description

Turbulence observations are based primarily on the nationwide aircraft-voice turbulence reports from 2022 to 2024 collected by China's civil-aviation authorities. After quality control (invalid records removed), 12,539 valid samples remain, each including the time, altitude, intensity (light–severe), and location of the turbulence encounter. Although such reports are subject to pilot-originated subjectivity, they remain an essential source for documenting real turbulence events. To improve the positional accuracy, this study uses Automatic Dependent Surveillance–Broadcast (ADS-B) track data (containing time, latitude, longitude, and altitude) to refine the spatial positioning of each reported event; records are matched by flight number and turbulence time to yield more objective and precise locations. In addition, key upper-air meteorological parameters wind field, geopotential height, temperature, and relative humidity are obtained from the European Centre for Medium-Range Weather Forecasts ERA5 reanalysis at $0.25^\circ \times 0.25^\circ$ horizontal resolution and 1 h temporal resolution. The vorticity used refers to the vertical component of relative vorticity, and divergence refers to the divergence of the horizontal wind field.

2.2. MOS CAT Turbulence Factor

The MOS CAT probability forecast factor is an advanced aviation meteorological forecasting tool that fully utilizes the output statistics (Model Output Statistics, MOS) technique of the Non-Hydrostatic Model (NGM) from the National Centers for Environmental Prediction (NCEP) in the United States. The core of this probability forecasting method lies in establishing a statistical correlation between the historical numerical model outputs and actual observed clear-air turbulence (CAT) events. By analyzing a large amount of historical data, this method can identify statistical patterns between specific parameter combinations in the model output and the probability of CAT events occurring. Based on these historical statistical relationships, the MOS CAT probability forecast factor can objectively predict the probability of CAT occurrences in specific areas in the future, providing important meteorological support for aviation safety. MOS CAT, the turbulence prediction factor, is computed from reanalysis data using the following formula:

$$\mathrm{DSH} = \frac{\partial \mathrm{v}}{\partial \mathrm{x}} + \frac{\partial \mathrm{u}}{\partial \mathrm{y}} \quad (1)$$

$$\mathrm{DST} = \frac{\partial u}{\partial x} - \frac{\partial v}{\partial y} \tag{2}$$

$$\mathrm{DEF} = \left(\mathrm{DSH}^2 + \mathrm{DST}^2\right)^{\frac{1}{2}} \tag{3}$$

$$\mathrm{MOS} = |\mathrm{V}|\mathrm{DEF} \tag{4}$$

where V is the horizontal wind speed, DSH denotes shear deformation, DST represents stretching deformation, and DEF is defined as the total deformation of the atmospheric wind field in that layer.

3. Results and Discussion

3.1. Altitude Distribution of Turbulence Reports

The aircraft voice report analysis from 2022 to 2024 (Figure 1a) shows that the altitude distribution characteristics of turbulence events within the China region are significant. Turbulence is mainly concentrated in the 3000–8000 m altitude layer (accounting for 61.0% of the total), with 7000–8000 m as the peak area. Within this layer, turbulence intensity is predominantly Light–Medium and Medium. The report proportion for the 7000–11,000 m altitude layer is 39.2%, and the proportion of Medium–Severe turbulence increased. Reports in regions below 3000 m and above 12,000 m are significantly reduced (both <200 times). This vertical distribution pattern indicates that aviation turbulence within China is predominantly active from the middle-upper troposphere to the lower stratosphere, consistent with the main cruising altitude range [10].

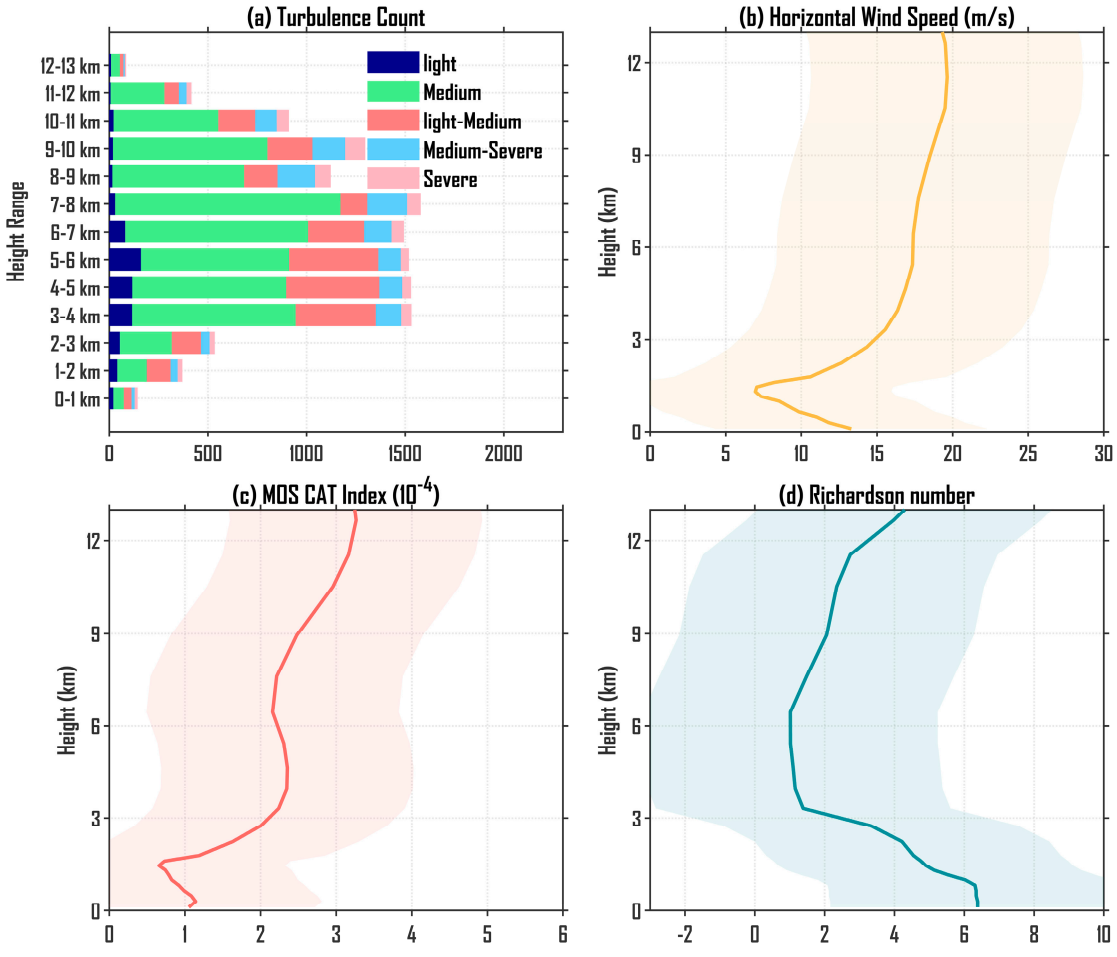

Figure 1. Vertical distributions of (**a**) turbulence–report height frequency and China–area averages of (**b**) horizontal wind speed, (**c**) MOS CAT index, and (**d**) Richardson number from 2022 to 2024.

The vertical profiles of key meteorological parameters (Figure 1b–d) reveal the background conditions associated with the turbulence distribution. Horizontal wind speed (Figure 1b) increases with height, peaking at ~12,000 m and corresponding to a typical upper-level jet. Notably, in the 3000–8000 m layer where turbulence is most frequent, the core region of the low-level jet, both wind speed and its vertical gradient ($\partial U/\partial z$) change markedly, and Figure 1d shows that the Richardson number (Ri) reaches its lowest point in this height range (a minimum value of -0.88, indicating significant instability), readily triggering Kelvin–Helmholtz instability (KHI) and fostering turbulence generation. The MOS CAT index (Figure 1c) remains elevated in both the upper-level jet region and the 3000–6000 m turbulence-prone layer, indicating high turbulence risk from strong vertical wind shear and unstable airflow. Although parameter intensities in the 6000–9000 m layer are slightly weaker, a certain degree of instability persists, consistent with the proportion of turbulence reports in that layer.

3.2. Seasonal Differences in Turbulence-Report Altitude Distribution

Figure 2 presents the seasonal characteristics of the altitude distribution of aircraft turbulence reports and the vertical profiles of key meteorological factors over China from 2022 to 2024. The analysis shows that the occurrence frequency of turbulence exhibits pronounced seasonal differences: winter (4193 reports, 33.4% of the annual total) and spring are the most frequent, concentrating mainly in the mid-to-upper levels (above 3000 m); summer (2632 reports, 21.0%) is dominated by low-altitude turbulence (0–6000 m), with the proportion in the lowest layer (0–3000 m) being particularly prominent; autumn has the lowest frequency, the widest altitude range (0–12,000 m), yet the weakest intensity (on average 188.6 reports per 1000 m) [11–13].

The seasonal patterns of turbulence distribution are governed by the synergistic action of upper-level jet dynamic forcing and thermal stratification. In winter, a classic stratification readily forms strong dynamic instability aloft and strong thermal stability below. The year's strongest upper-level jet (>30 m s^{-1}) and its accompanying extreme vertical horizontal wind shear, in addition to the smaller Ri numbers at the higher levels, driving the largest annual MOS CAT index, dominate the elevated turbulence risk in the mid-to-upper layer (3000–10,000 m, accounting for 85.7% of winter reports); dynamic instability is the core driver [5,14–16]. In autumn, the turbulence risk contracts and concentrates in the mid-upper layer (4000–9000 m, 58.7%). Horizontal wind speed and the MOS CAT index are all markedly stronger than in summer, with a narrowed vertical range, indicating that upper-level turbulence potential is more focused and more dependent on strong wind shear for dynamic forcing, while thermo-dynamic instability in the mid-lower layer weakens. In spring, the clear-air turbulence potential in the mid-upper layer (10,000–11,000 m) arises mainly from strong wind shear under jet dynamic forcing superimposed on a thermally unstable upper-level layer [17]; the mid-layer (4000–6000 m) also retains relatively high wind-shear risk. The prominent low-level (0–6000 m) turbulence risk in summer is chiefly attributed to active thermal convection within the boundary layer and the frequent deep convective precipitation in summer [11]. Overall, the horizontal wind speed, wind shear, and MOS CAT index intensities are significantly lower than in other seasons, and the role of dynamic instability is reduced.

Overall, the altitude distribution of aircraft turbulence over China exhibits pronounced seasonal contrasts: high-altitude turbulence (9000–12,000 m) persists year-round, driven mainly by vertical horizontal wind shear; low-level turbulence risk is significant only in summer and closely tied to thermal convection; the vertical contraction of turbulence risk in autumn and winter is directly coupled to the seasonal evolution of jet-stream intensity.

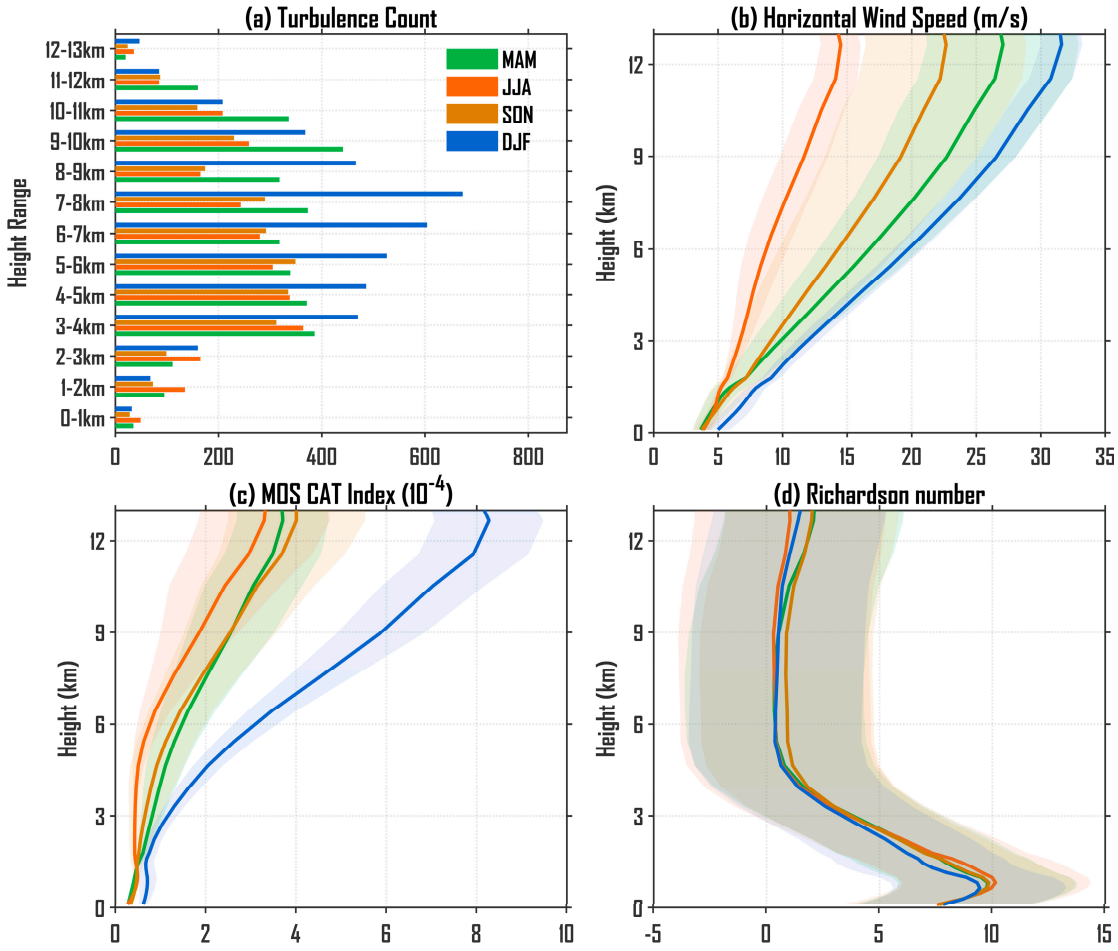

Figure 2. Seasonal differences in (**a**) turbulence–report altitude distribution and China–area mean vertical profiles of (**b**) horizontal wind speed, (**c**) MOS CAT index, and (**d**) Richardson number from 2022 to 2024.

3.3. Spatial Distribution of Turbulence Reports

During the period from 2022 to 2024, the frequency of aircraft turbulence events across China shows pronounced spatial heterogeneity (Figure 3a). The Central-South and Southwest regions are the two core high-incidence areas, with occurrence frequencies far exceeding those of other regions (about 2900 times for Central-South and about 2800 times for Southwest). Secondly, Xinjiang has experienced a total of about 2000 occurrences. North China and Northwest China exhibit similar frequencies, all exceeding 1000 times, whereas Northeast China records the lowest frequency (about 450 times). This distribution pattern clearly indicates that the mid-upper tropospheric dynamic environments, especially the 5000–6000 m layer where turbulence is most frequent, differ markedly among China's subregions, with Central-South and Southwest China presenting the most complex and unstable atmospheric conditions that readily trigger turbulence. Therefore, this study uses the 600–400 hPa averaged physical fields to analyze how the atmospheric dynamic structure of this key layer influences the spatial distribution of turbulence.

The formation of the high-incidence zones in Central-South and Southwest China is closely linked to the specific atmospheric dynamic structure of the 600–400 hPa layer (Figure 3b–d). Strong vorticity gradient and dynamic instability: This region (especially Central and Southwest China) shows marked positive vorticity, with a local vorticity maximum in the Southwest and a strong vorticity gradient nearby (e.g., toward South China) (Figure 3b). This steep gradient is a key background for mesoscale disturbances and vortex generation, readily triggering small-scale perturbations and turbulent patches,

such as Kelvin–Helmholtz instability (KHI) [18], and forming intense wind-shear bands that directly trigger turbulence. Alternating divergence and vertical perturbations: The divergence field over Central-South and Southwest China (especially in areas with drastic terrain changes) presents clear alternating positive and negative centers (Figure 3c). This "noisy" signal may indicate small-scale divergence/convergence generated by gravity wave activities triggered by the terrain, which can directly induce oscillations in vertical movement and may exacerbate local wind shear, thereby providing favorable dynamic conditions for the generation of turbulence. This pattern of vertical perturbations causes unstable fluctuations at flight altitudes [19]. Mid-level jet shear: The wind field shows a mid-level jet axis over 25–35° N, 105–120° E with a core speed exceeding 12 m s^{-1} (locally up to 16 m s^{-1} in Central China) (Figure 3d). Its left flank, characterized by a marked wind-speed gradient, exactly covers the Central-South to Southwest high-incidence zone, spatially coinciding with the turbulence maxima. The strong shear of the jet supplies continuous energy for turbulence generation.

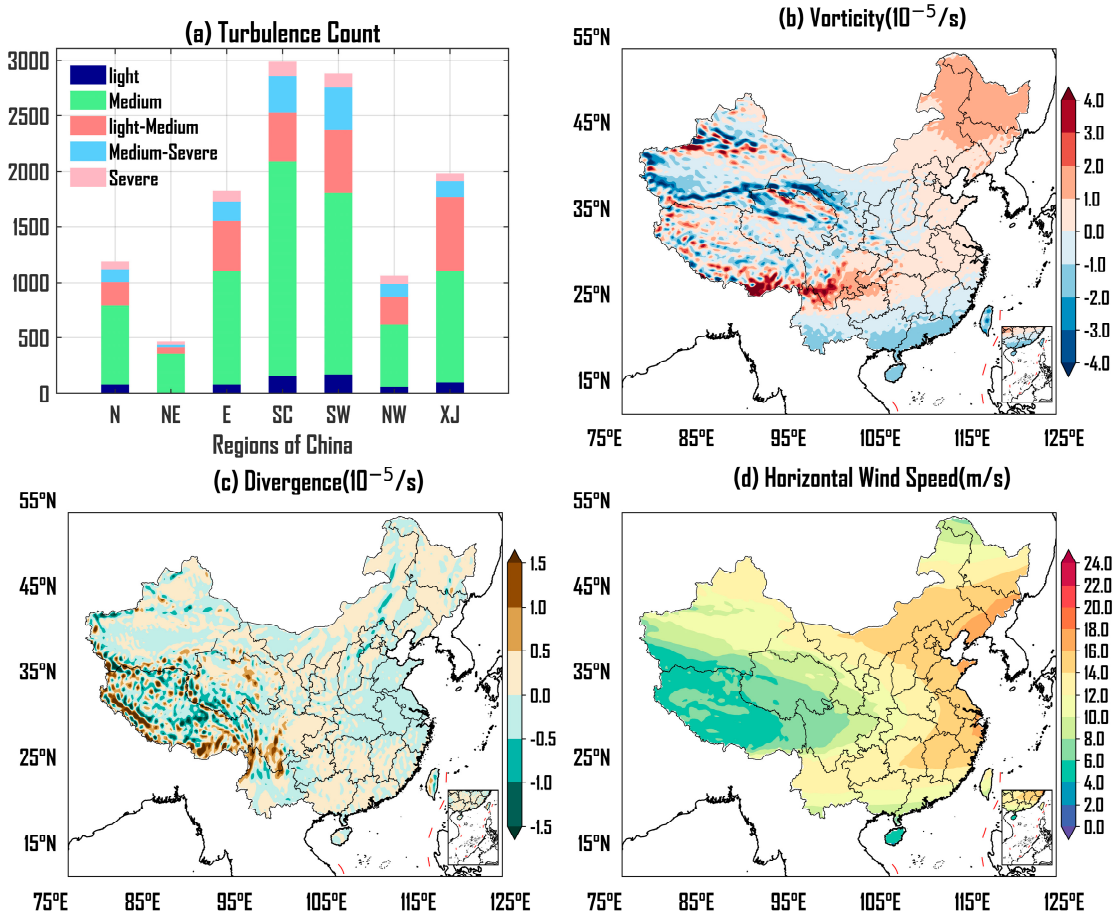

Figure 3. (**a**) Aircraft turbulence event frequency by region in China and 600–400 hPa mean fields for (**b**) vorticity, (**c**) divergence, and (**d**) horizontal wind speed during the period from 2022 to 2024.

In summary, the prominence of Central-South and Southwest China as turbulence hotspots is not coincidental; it is the joint outcome of the strong vorticity gradient, alternating divergence perturbations, and mid-level jet shear within that layer. Together, these elements create a typical turbulence-prone environment marked by pronounced dynamic instability and frequent vertical disturbances.

3.4. Winter Characteristics of the Spatial Distribution of Turbulence Reports

Winter is the peak season for aircraft turbulence events in China. An analysis of the winter 2022–2024 spatial distribution (Figure 4a) shows that the Southwest and Central-South regions, especially Central China, remain the core high-incidence zones, with frequencies markedly higher than elsewhere in the country. This pattern highlights the critical influence of winter-specific atmospheric circulation on flight stability. To uncover the dynamic causes, this study again focuses on the 600–400 hPa layer (corresponding to the altitude band where turbulence is most frequent) and examines the vorticity, divergence, and horizontal wind-field features within this layer.

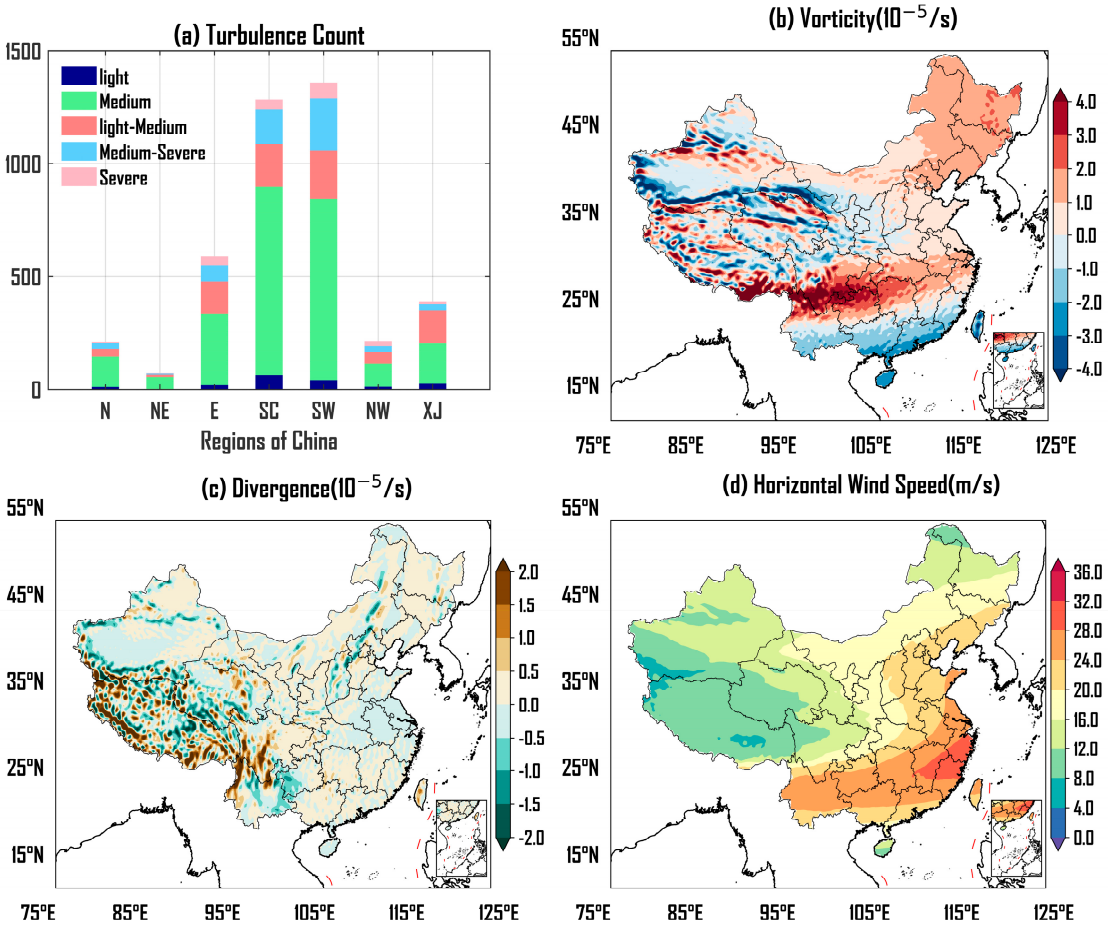

Figure 4. (**a**) Winter 2022–2024 aircraft turbulence event frequency by region in China and 600–400 hPa mean fields of (**b**) vorticity, (**c**) divergence, and (**d**) horizontal wind speed.

The formation of the winter high-incidence zones can be attributed to the marked intensification and synergistic interaction of dynamical perturbations within this layer (Figure 4b–d). The positive-vorticity maximum over the southwest expands in both area and strength (core value $> 5 \times 10^{-5}$ s^{-1}) and extends southeastward to northern South China, while a distinct positive-vorticity belt forms over Central China; along the edges, especially along the Southwest-South China boundary, the greatly sharpened vorticity gradient creates a belt of dynamical instability that readily excites small-scale vortices and wind-field perturbations (e.g., Kelvin–Helmholtz waves), generating intense local wind shear [15,18,20]. Over Central-South and Southwest China, the divergence field displays a more pronounced alternating pattern of positive and negative centers; the frequent alternation between horizontal divergence and convergence strongly drives vertical-motion perturbations, causing violent fluctuations at flight levels. In addition, the mid-level jet

shifts markedly southward (main axis ~22–30° N) and forms a strong jet streak (core wind speed > 32 m s^{-1}); the turbulence-prone left flank of the jet covers the area from Central China to northern Southwest China, perfectly overlapping the high-incidence zone. Between 105° and 120° E, strong vertical wind shear continuously supplies energy for turbulence development and, coupled with vorticity/divergence perturbations, further amplifies instability. Through the coordinated action of these multiscale dynamical processes, a strongly turbulence-prone environment is created in the winter mid-upper troposphere.

In summary, within the winter mid-troposphere, the intensified vorticity gradient drives small-scale dynamic instability, the amplified divergence perturbations trigger marked vertical-motion changes, and the south-shifted strong jet supplies the background energy and shear forcing. Acting together, these three factors create a highly non-uniform environment of intense dynamic perturbations over Southwest and Central-South China, establishing a typical high-turbulence-risk zone that is the core reason for frequent turbulence this season. This understanding provides an important scientific basis for identifying high-risk airspace and for flight-warning planning.

4. Conclusions

This study systematically analyzed Chinese aircraft turbulence reports together with ERA5 reanalysis data from 2022 to 2024 and, for the first time, revealed the multi-scale physical causes of turbulence over China. The results show a distinctive bimodal vertical structure in the country's airspace: a primary peak at 3000–8000 m (61.0% of reports, mostly moderate), closely linked to strong vertical horizontal wind shear and Kelvin–Helmholtz instability (KHI) turbulence within the low-level jet core, and a secondary peak at 7000–11,000 m (39.2%, with a higher fraction of moderate-to-severe cases) that corresponds to a dynamically unstable upper-level stratification. Seasonal variation is pronounced: winter accounts for 33.4% of annual reports and forms a classic "unstable aloft, stable below" stratification driven by strong upper-level jets (>30 m s^{-1}) and extreme wind shear, while summer (21.0%) is dominated by low-level thermally driven convection, and spring and autumn represent transitional regimes modulated by jet-stream intensity.

Spatially, Central-South and Southwest China are the main turbulence hotspots, arising from the combined action of three mid-level (600–400 hPa) dynamic factors: a strong vorticity gradient (reaching 4×10^{-5} s^{-1} in the southwest) that excites turbulent patches, alternating divergence perturbations that cause rapid changes in vertical motion, and mid-level jet shear (core > 12 m s^{-1}) that continuously supplies turbulence energy. In winter, these features intensify: the jet shifts south to 22–30° N, and the vorticity strengthens (>5×10^{-5} s^{-1} extending into South China), markedly amplifying the turbulence risk. This study establishes a dynamic thermal coupling framework that offers a new perspective on the formation mechanisms of aircraft turbulence in the context of complex terrain and monsoon influences.

The findings not only deepen the understanding of how aviation turbulence forms but can also be directly applied to aviation safety warning systems to improve forecast accuracy and provide a scientific basis for dynamic route planning. Future research should integrate climate models to further assess the long-term impact of global warming on turbulence risk, offering theoretical support for the sustainable development of the aviation sector.

Author Contributions: Conceptualization, W.Z. and T.Y.; methodology, W.Z.; software, X.Z.; validation, W.Z., X.Z. and W.Y.; formal analysis, W.Z.; investigation, W.Z.; resources, W.Z.; data curation, W.Z.; writing—original draft preparation, W.Z.; writing—review and editing, W.Z., X.Z., W.Y., C.Z., M.H. and T.Y.; visualization, W.Z.; supervision, T.Y.; project administration, W.Z.; funding acquisition, X.Z. All authors have read and agreed to the published version of the manuscript.

Funding: This work was supported by National Key Research and Development Program of China (No. 2022YFC3002502).

Institutional Review Board Statement: Not applicable.

Informed Consent Statement: Not applicable.

Data Availability Statement: The raw pilot reports (PIREPs) data used in this study are subject to licensing agreements with the data provider and are not publicly archived. However, the data can be made available upon reasonable request from the corresponding author, T. Yang (tingyang@mail.iap.ac.cn).

Conflicts of Interest: The authors declare no conflict of interest.

References

1. Kim, J.-H.; Chun, H.-Y. Statistics and Possible Sources of Aviation Turbulence over South Korea. *J. Appl. Meteorol. Climatol.* **2011**, *50*, 311–324. [CrossRef]
2. Storer, L.N.; Williams, P.D.; Gill, P.G. Aviation Turbulence: Dynamics, Forecasting, and Response to Climate Change. *Pure Appl. Geophys.* **2019**, *176*, 2081–2095. [CrossRef]
3. Williams, J.K. Using Random Forests to Diagnose Aviation Turbulence. *Mach. Learn.* **2014**, *95*, 51–70. [CrossRef] [PubMed]
4. Koch, P.; Wernli, H.; Davies, H.C. An Event-Based Jet-Stream Climatology and Typology. *Int. J. Climatol.* **2006**, *26*, 283–301. [CrossRef]
5. Williams, P.D. Increased Light, Moderate, and Severe Clear-Air Turbulence in Response to Climate Change. *Adv. Atmos. Sci.* **2017**, *34*, 576–586. [CrossRef]
6. Sharman, R. Nature of Aviation Turbulence. In *Aviation Turbulence: Processes, Detection, Prediction*; Sharman, R., Lane, T., Eds.; Springer: Cham, Switzerland, 2016; pp. 3–30. [CrossRef]
7. Jaeger, E.B.; Sprenger, M. A Northern Hemispheric Climatology of Indices for Clear Air Turbulence in the Tropopause Region Derived from ERA40 Reanalysis Data. *J. Geophys. Res. Atmos.* **2007**, *112*, D20106. [CrossRef]
8. Wu, G.; Zhou, X.; Xu, X.; Huang, J.; Duan, A.; Yang, S.; Hu, W.; Ma, Y.; Liu, Y.; Bian, J.; et al. An Integrated Research Plan for the Tibetan Plateau Land–Air Coupled System and Its Impacts on the Global Climate. *Bull. Am. Meteorol. Soc.* **2023**, *104*, E158–E177. [CrossRef]
9. Zhao, P.; Xu, X.; Chen, F.; Guo, X.; Zheng, X.; Liu, L.; Hong, Y.; Li, Y.; La, Z.; Peng, H.; et al. The Third Atmospheric Scientific Experiment for Understanding the Earth–Atmosphere Coupled System over the Tibetan Plateau and Its Effects. *Bull. Am. Meteorol. Soc.* **2018**, *99*, 757–776. [CrossRef]
10. Li, K.; Chen, X.; A, L.; Wu, K.; Liu, H.; Dai, F.; Yang, T.; Yu, J.; Wang, K. Analysis of the Relationship between Upper-Level Aircraft Turbulence and the East Asian Westerly Jet Stream. *Atmosphere* **2024**, *15*, 1138. [CrossRef]
11. Cai, X.; Wan, Z.; Wu, W.; Yang, B.; Yi, Z. An Ensemble Prediction Method of Aviation Turbulence Based on the Energy Dissipation Rate. *Chin. J. Atmos. Sci.* **2023**, *47*, 1085–1098.
12. Zhang, L.; Sun, H.; Wang, C.; Yu, C.; Lu, B. Spatiotemporal Pattern of Air Turbulence Risks with QAR Flight Big Data. *Geomat. Inf. Sci. Wuhan Univ.* **2024**, *49*, 482–490. [CrossRef]
13. Ko, H.-C.; Chun, H.-Y.; Bechtold, P. Evaluation and Improvement of the ECMWF Aviation Turbulence Forecasts. *J. Geophys. Res. Atmos.* **2025**, *130*, e2024JD043158. [CrossRef]
14. Chen, L.; Tan, B.; Kvamstø, N.G.; Johannessen, O.M. Wintertime Cyclone/Anticyclone Activity over China and Its Relation to Upper Tropospheric Jets. *Tellus A Dyn. Meteorol. Oceanogr.* **2014**, *66*, 21889. [CrossRef]
15. Li, K.; Wu, K.; Liu, H.; Xu, W.; Li, G.; Yang, Z.; Liu, G.; Dong, B. Spatiotemporal Distribution Patterns of Turbulence on Major High-Altitude Aircraft Routes in China. *Trans. Atmos. Sci.* **2024**, *47*, 789–797. [CrossRef]
16. Wang, L.; Huang, R.; Gu, L.; Chen, W.; Kang, L. Interdecadal Variations of the East Asian Winter Monsoon and Their Association with Quasi-Stationary Planetary Wave Activity. *J. Clim.* **2009**, *22*, 4860–4872. [CrossRef]
17. Knox, J.A.; McCann, D.W.; Williams, P.D. Application of the Lighthill–Ford Theory of Spontaneous Imbalance to Clear-Air Turbulence Forecasting. *J. Atmos. Sci.* **2008**, *65*, 3292–3304. [CrossRef]
18. Sharman, R.D.; Trier, S.B.; Lane, T.P.; Doyle, J.D. Sources and Dynamics of Turbulence in the Upper Troposphere and Lower Stratosphere: A Review. *Geophys. Res. Lett.* **2012**, *39*, L12803. [CrossRef]

19. Wolff, J.K.; Sharman, R.D. Climatology of Upper-Level Turbulence over the Contiguous United States. *J. Appl. Meteorol. Climatol.* **2008**, *47*, 2198–2214. [CrossRef]
20. Lane, T.P.; Doyle, J.D.; Plougonven, R.; Shapiro, M.A.; Sharman, R.D. Observations and Numerical Simulations of Inertia–Gravity Waves and Shearing Instabilities in the Vicinity of a Jet Stream. *J. Atmos. Sci.* **2004**, *61*, 2692–2706. [CrossRef]